UNCLASSIFIED

AD NUMBER

AD815788

NEW LIMITATION CHANGE

TO

Approved for public release, distribution
unlimited

FROM

Distribution authorized to U.S. Gov't.
agencies and their contractors;
Administrative/Operational Use; MAR 1967.
Other requests shall be referred to
Ballistic Research Laboratoriess, Aberdeen
Proving Ground, MD 21005.

AUTHORITY

ARLS/CI, 23 Sep 2005

THIS PAGE IS UNCLASSIFIED

BRL

AD

MEMORANDUM REPORT NO. 1833

AERODYNAMIC CHARACTERISTICS OF

THE 7.62 MM NATO AMMUNITION M-59, M-80, M-61, M-62

by

Maynard J. Piddington

March 1967

U. S. ARMY MATERIEL COMMAND
BALLISTIC RESEARCH LABORATORIES
ABERDEEN PROVING GROUND, MARYLAND

D D C
RECEIVED
JUN 26 1967
C

Destroy this report when it is no longer needed.
Do not return it to the originator.

BALLISTIC RESEARCH LABORATORIES

MEMORANDUM REPORT NO. 1833

MARCH 1967

AERODYNAMIC CHARACTERISTICS OF THE 7.62 MM NATO AMMUNITION M-59, M-80, M-61, M-62

Maynard J. Piddington

Exterior Ballistics Laboratory

ABERDEEN PROVING GROUND, MARYLAND

BALLISTIC RESEARCH LABORATORIES

AERODYNAMIC CHARACTERISTICS OF THE 7.62 MM NATO AMMUNITION M-59, M-80, M-61, M-62

ABSTRACT

Tests have been conducted in the Free-Flight Aerodynamic Range on the NATO family of ammunition (M-80 ball, M-59 ball, M-62AP, and M-61 tracer). This report is the presentation and discussion of the data obtained in these tests. In general, the projectiles exhibited adequate gyroscopic and dynamic stability in the regions of probable use. The non-tracer members appear to have sufficiently similar drag properties to be adequate ballistic matches, while the tracer is not a match beyond about 600 meters.

TABLE OF CONTENTS

LIST OF SYMBOLS

d   Maximum body diameter of projectile

q   Angular velocity

s $\dfrac{8\pi I_x^2}{I_y N^2 \rho d^5 C_{M_\alpha}}$ (Stability factor)

M   Mach Number

N   Barrel twist

S $\pi d^2/4$

V   Missile velocity

C_D $\dfrac{\text{Drag Force}}{(1/2)\rho V^2 S}$

C_{M_α} $\dfrac{\text{Static Moment}}{(1/2)\rho V^2 S\ell\alpha}$

$*C_{M_{p\alpha}}$ $\dfrac{\text{Magnus Moment}}{(1/2)\rho V^2 S\ell \frac{q\ell}{V}\alpha}$

$*C_{M_q} + C_{M_{\dot\alpha}}$ $\dfrac{\text{Damping Moment}}{(1/2)\rho V^2 S\ell \frac{q\ell}{V}}$

C_{N_α} $\dfrac{\text{Normal Force}}{(1/2)\rho V^2 S\alpha}$

---

* A negative $C_{M_q} + C_{M_{\dot\alpha}}$ indicates that the moment opposes the angular velocity and a positive $C_{M_{p\alpha}}$ indicates that the Magnus moment is trying to rotate the missile's nose about the velocity vector in the direction of spin.

7

LIST OF SYMBOLS (Continued)

CP_N	Center of pressure of the normal force
I_x	Axial moment of inertia
I_y	Transverse moment of inertia
α	Angle of attack
$\overline{\delta^2}$	Mean squared yaw
ℓ	Reference length ($\ell = d = 0.308$ inch)
ρ	Air density

I. INTRODUCTION

The adoption of the 7.62 mm NATO infantry weapon series has led to the introduction of a new family of small arms projectiles: the M-80 ball, the M-59 alternate ball, the M-61 armor piercing, and the M-62 tracer. In addition to their use in the infantry rifle, other applications for the ammunition were proposed that involved more severe flight conditions; for example, the U.S. Air Force proposed the development of a Gatling-type gun for use in light aircraft and for fighters of the century class, and the U.S. Army proposed several uses for helicopter armament. Proper evaluation of such uses required more aerodynamic data for the projectiles than had previously been obtained. To fill this need, the Air Proving Ground Center at the Eglin Air Force Base, Florida, requested that the Ballistic Research Laboratories (BRL) undertake spark range tests with the four types of ammunition.[*] Applications of the data obtained have been reported.[1][**] BRL enlarged the basic program to insure that adequate information was obtained to evaluate a wide spectrum of uses.

II. TEST

The shapes of the four types of projectiles are shown in Figure 1. The shapes depicted are a synthesis obtained from consideration of drawings of the projectiles and from physical measurements[2] of actual unfired projectiles.[***] Typical physical properties are given in Table I. The four projectiles have the same ogival nose, and all but the M-62 tracer have similar boattailed afterbodies (the M-62 has a rounded base). The alternate ball M-59 and the AP M-61 appear to be identical in general exterior contour, while the ball M-80 is about one-half caliber shorter

---

[*] *This was done in compliance with MIPR NR-4-17, Project Nr. 5845.*

[**] *Superscript numbers denote references which may be found on page 23.*

[***] *A more accurate determination of the physical dimensions should be obtained by measuring the projectiles after launch. To do this, the projectile should be launched at standard velocity and then recovered without damage caused by the recovery system.*
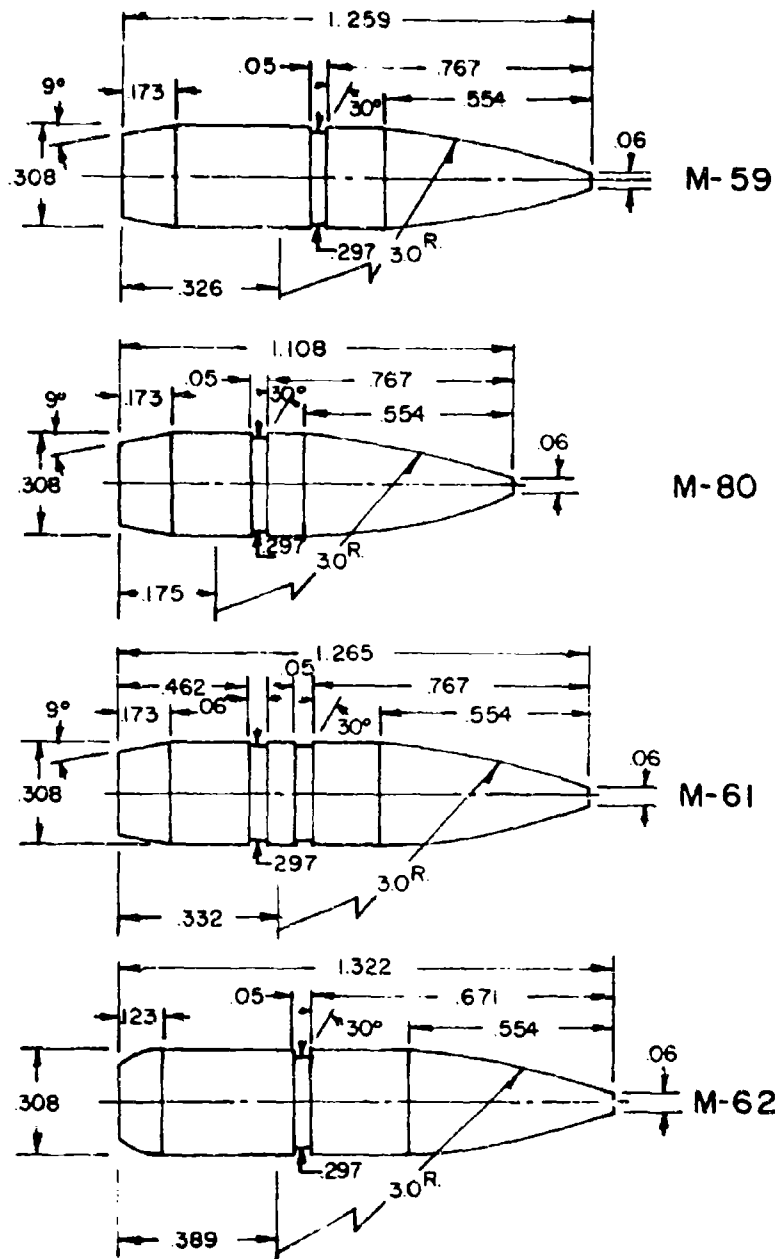
Figure 1. Shapes and dimensions of NATO ammunition

Table I. Physical Properties Of NATO Ammunition

Projectile	Diameter (inches)	Length (inches)	Mass (grams)	Center of Mass (inches from base)	Moments of Inertia Axial $gm-in^2$	Transverse $gm-in^2$
M-80	.308	1.108	9.444	.491	.0765	.6.5
M-59	.308	1.259	9.627	.511	.0975	.965
M-61	.308	1.235	9.552	.509	.0934	.5795
M-62	.308	1.322	9.035	.402	.0918	.75

11

than the other two. All types have a knurled groove at about the same distance from the nose tip and the M-61 has a second beveled groove aft of the knurled one.

The projectiles were all tested in the BRL Aerodynamics Range.[3] The M-14 rifle was used to launch the rounds at 2850 ft per sec (standard muzzle velocity) and at velocities reduced to about 1200 ft per sec. The M-80 firings were extended into the subsonic region. Higher than normal velocities were obtained by using a Mann barrel* but the muzzle velocity was limited to less than 3300 ft per sec because of extensive damage to the projectile above this velocity.

All data were computed in the usual manner[4] and are given in Table II; plots of these calculations are presented in the Appendix. It is noted that the experimental data for the M-62 were obtained in the same manner as for the other three types.

Photographs of each type of projectile are shown in Figures 2 through 6. Figures 5 and 6 are shadowgraph pictures of the inert M-62 and the M-62 with tracer respectively. The difference in the nature of the flow in the area of the wake on the two pictures should be noted. This difference in the wake flow accounts for the major decrease in drag when the tracer is burning. A slight but undetermined drag decrease can be attributed to the thrust of the tracer.

III. RESULTS

A. Drag

The drag force coefficient, C_D, for each round is obtained by fitting the time-distance data to a cubic equation by a least squares process. (At about Mach one, where the drag is changing quite rapidly,

---

*The normal twist of 1-14 rifles is 1 turn in 12 inches and for the Mann barrel used it is 1 turn in 10 inches. A 1 in 12 inch twist gun may allow a slightly higher velocity before projectile damage is excessive.

12

Table II. Summary Of Aerodynamic Properties

M-59

Range Rd.	M	$\sqrt{\overline{\delta^2}}$ (deg.)	C_D	C_{M_α}	$C_{M_q} + C_{M_{\dot\alpha}}$	$C_{M_{p\alpha}}$	C_{N_α}	CP_N (inches from base)	s
6549	2.785	4.5	.316	2.31	-5.6	.14	2.8	.760	2.19
6548	2.776	2.7	.300	2.36	-5.8	.13	2.5	.800	2.20
6462	2.410	2.2	.323	2.48	-6.1	.16	2.6	.803	1.52
6463	2.393	3.2	.322	2.41	-6.0	.17	2.7	.786	1.47
6490	1.813	6.5	.425	2.50	-5.3	.10	3.5	.733	1.30
6884	1.797	3.4	.372	2.58	-5.0	.04	2.9	.787	1.32
6881	1.795	5.8	.416	2.57	-6.3	.15	2.8	.798	1.34
6903	1.299	9.3	.536	2.67	-4.3	.04	2.8	.799	1.20
6901	1.267	6.9	.482	2.68	-3.0	-.04	2.6	.826	1.18
6910	1.132	11.0	.596	2.72	-4.0	-.02	2.7	.820	1.23
6907	1.131	10.9	.592	2.72	-2.8	-.06	2.8	.808	1.18

Table II. Summary Of Aerodynamic Properties (Continued)

M-80

Range Rd.	M	$\sqrt{\bar{\delta^2}}$ (deg.)	C_D	C_{M_α}	$C_{M_q} + C_{M_{\dot\alpha}}$	$C_{M_{p\alpha}}$	C_{N_α}	CP_N (inches from base)	s
6547	2.769	3.2	.297	1.74	-3.6	-.08	2.5	.643	3.33
6546	2.744	4.0	.309	1.80	-3.6	-.04	2.6	.641	3.30
6584	2.516	5.6	.350	1.80	-3.5	.04	2.7	.634	2.44
6583	2.464	5.2	.330	1.77	-3.3	.03	2.8	.626	2.22
6158	2.448	.6	.290	1.81	-2.8	-.21	2.6	.647	2.08
6159	2.445	.6	.294	1.79	-4.5	-.19	2.0	.712	2.14
6464	2.410	7.1	.390	1.86	-3.6	.03	3.0	.626	2.35
6491	1.943	3.5	.370	1.94	-2.8	-.08	2.8	.648	2.07
6492	1.867	2.3	.356	1.87	-3.6	-.06	2.6	.649	2.00
6494	1.695	4.6	.408	1.95	-4.2	.08	2.8	.646	1.96
6493	1.615	3.1	.400	1.92	-4.9	.05	2.6	.658	1.91
6543	1.402	4.1	.439	1.97	-3.3	.01	2.7	.659	1.99
6542	1.378	4.6	.446	1.98	-2.9	-.04	2.5	.673	1.89
6530	1.330	5.7	.470	2.04	-2.6	-.03	2.6	.658	1.93
6529	1.295	3.6	.445	2.03	-2.2	-.10	2.4	.689	1.88
6528	1.001	5.4	.476	2.11	-1.5	-.09	2.4	.705	1.82
6528	.976	5.3	.394	--	--	--	--	--	--
6528	.954	4.8	.314	2.44	3.0	.02	2.5	.737	1.70
6527	.946	6.7	.310	--	--	--	--	--	--

Table II. Summary Of Aerodynamic Properties (Continued)

M-80

Range Rd.	M	$\sqrt{\overline{\delta^2}}$ (deg.)	C_D	C_{M_α}	$C_{M_q} + C_{M_{\dot\alpha}}$	$C_{M_{p\alpha}}$	C_{N_α}	CP_N (inches from base)	s
6737	.637	5.7	.192	2.11	2.4	-.30	1.91	--	--
6738	.635	7.0	.210	2.14	- .4	-.07	1.81	--	--
6740	.606	10.1	.284	1.73	--	--	2.36	--	--
6739	.594	2.8	.144	2.13	- .8	-.10	1.65	--	--
6740	.585	14.2	.360	2.02	--	--	2.08	--	--
6735	.565	13.5	.364	2.05	2.6	-.37	1.97	--	--
6736	.529	8.0	.266	1.74	--	--	2.18	--	--

Table II. Summary Of Aerodynamic Properties (Continued)

M-61

Range Rd.	M	$\sqrt{\overline{\delta^2}}$ (deg.)	C_D	C_{M_α}	$C_{M_q} + C_{M_{\dot\alpha}}$	$C_{M_{p\alpha}}$	C_{N_α}	CP_N (inches from base)	s
6553	2.788	3.3	.316	2.24	-5.4	.15	2.8	.757	2.36
6552	2.753	1.0	.293	2.24	-4.5	.09	2.2	.821	2.26
6460	2.520	7.8	.380	2.34	-5.3	.14	3.2	.732	1.50
6461	2.459	4.2	.340	2.45	-5.8	.14	2.7	.786	1.42
6899	1.817	8.6	.483	2.59	-5.4	.09	3.2	.754	1.27
6882	1.725	4.9	.412	2.48	-6.1	.16	2.9	.769	1.35
6905	1.387	10.0	.553	2.62	-2.1	-.01	3.1	.767	1.22
6902	1.309	11.7	.608	2.53	-4.0	.03	3.0	.762	1.30

Table II.   Summary Of Aerodynamic Properties (Continued)

M-62

Range Rd.	M	$\sqrt{\overline{\delta^2}}$ (deg.)	C_D	C_{M_α}	$C_{M_q} + C_{M_{\dot\alpha}}$	$C_{M_{p\alpha}}$	C_{N_α}	CP_N (inches from base)	s
6551	2.849	1.7	.246	1.54	-6.2	.19	2.7	.776	3.12
6550	2.823	2.7	.252	1.52	-6.0	.24	2.8	.771	3.25
6458	2.510	4.9	.340	1.54	-6.0	.24	3.1	.755	2.26
6459	2.497	4.3	.336	1.52	-6.0	.20	3.0	.755	2.18
6900	1.854	7.7	.463	1.68	-6.6	.14	3.2	.769	2.11.
6883	1.731	7.1	.340	1.81	-6.5	.14	3.1	.779	2.00
6906	1.423	5.8	.486	1.94	-6.7	-.06	2.8	.824	1.83
6904	1.368	9.3	.560	1.90	-4.5	-.20	2.9	.808	1.82
6913	.917	12.8	.409	2.06	-4.6	-.37	2.7	.844	1.79
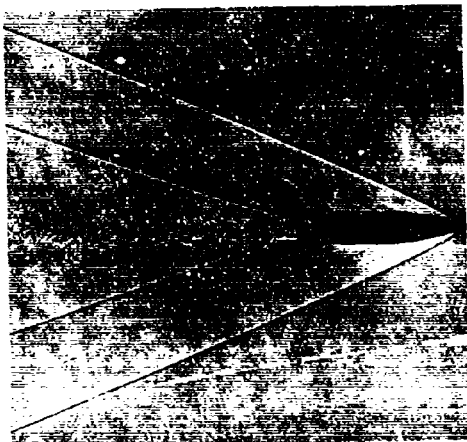
Figure 2. M-59 ball (M = 2.8)
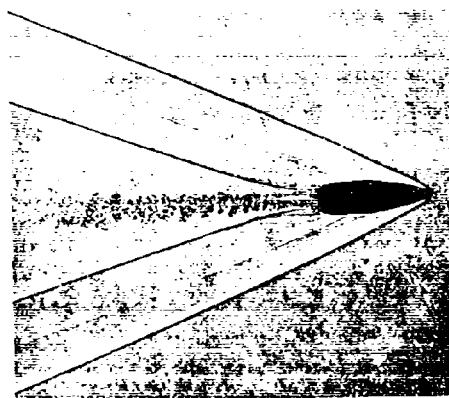
Figure 3. M-80 Ball (M = 2.8)
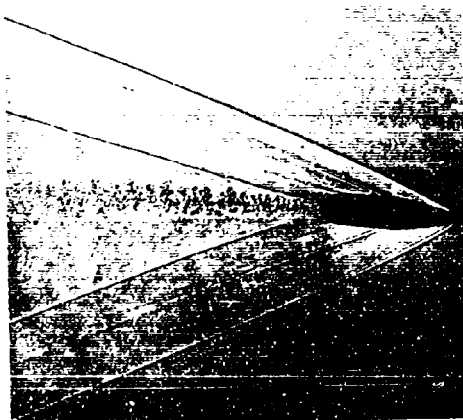
Figure 4. M-61 AP (M = 2.8)

18
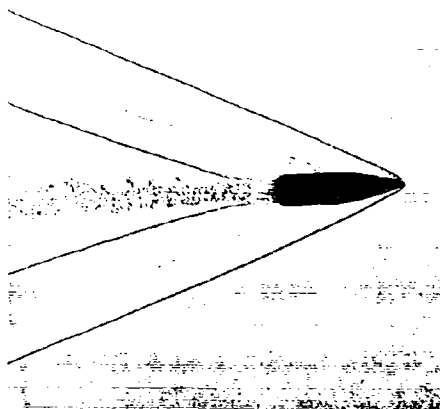
Figure 5. M-62 tracer (not burning)
(M = 2.8)
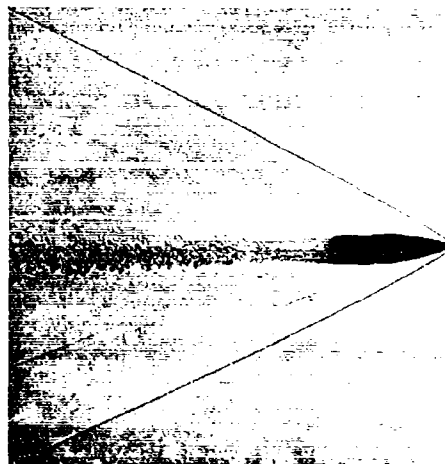
Figure 6. M-62 tracer (burning)
(M = 2.5)

it is necessary to divide the time-distance data into two parts and compute two drags. This was done on two M-80 rounds.) C_D is then reduced to zero yaw by the relationship:

$$C_D = C_{D_o} + C_{D_\delta 2} \overline{\delta^2}$$

The yaw drag coefficient, $C_{D_\delta 2}$, is normally obtained from a straight line fit of the C_D vs $\overline{\delta^2}$ data for a constant Mach number. This requires several data points at the same Mach number with varying amounts of yaw. Very often, also, $C_{D_\delta 2}$ is non-linear with yaw, due mainly to a separation of flow about the body. By using the subsonic M-80 data which had a wide variety of yaws and by close examination of the photographic plates it was possible to determine at what yaw level the flow separated. Once the flow separation was established, it was possible to determine

19

$C_{D_\delta 2}$ below and above that value of yaw. $C_{D_\delta 2}$ for the M-59 and M-61 above separation was assumed to be the same as that for the M-80. The values at the indicated yaw levels are listed below.

Yaw Drag Coefficient $(1/\text{rad}^2)$

M-80	M-59 and M-61
6.0 (0 to 8 deg)	6.0 (0 to 3 deg)
2.7 (> 8 deg)	2.7 (> 3 deg)

C_{D_o} is plotted in Figures A-1 and A-2 of the Appendix as a function of Mach number. The curves of the M-59 and the M-80 projectiles in the supersonic region are, for all practical purposes, identical; the drag of the M-61 projectile is about 10 percent higher. For these three projectiles, the nose and the boattail have identical shapes; therefore, the differences in drag are due either to body shape or to the phenomena of the flow about the projectile. Since the drag of the two ball ammunition is about the same, the drag due to body length (the M-59 being about 1/2 caliber longer) is negligible. On the other hand, the M-61, which has the same shape as the M-59, has a 10 percent higher drag. Evidently, this is due to the extra groove in the body which produces a more highly disturbed flow.

The drag of the tracer round is much more complicated. Two curves are shown in Figure A-2. These curves were obtained by close examination of the time-distance data for each round. The data for each round were divided into several increments, each containing only three timing observations. Drag values were then computed for each increment. An example of such a drag computation for a single round is shown in Figure A-3. The curve indicates a large change in drag in a relatively short period of time (about 0.07 seconds). This represents about 200 feet of travel at standard muzzle velocity before the tracer is in full operation. The upper curve is drawn through that portion of data for

each round represented by the ignition phase (non-burning). Using the data at the end of the range for each round, the bottom curve is a good approximation of the constant burning phase.

Caution should be exercised when computing the velocity history of the M-62 projectile. A round launched at a velocity of about 2850 ft per sec will initially have a drag which follows the upper curve in Figure A-2. When the tracer begins to burn, however, (about 65 feet from the gun) the drag drops very rapidly to the bottom curve where it remains until the tracer has burned out. At this point (about 1 - 1/2 seconds flight time), the drag jumps back to the upper curve where it will remain throughout the remaining portion of its trajectory.

B. Stability

The overturning moment derivative, C_{M_α}, and the sum of the damping moment derivatives, $C_{M_q} + C_{M_{\dot\alpha}}$, are plotted versus Mach number in Figures A-4 and A-5, respectively. Nothing unusual is evident in these curves; as one would expect, they have similar trends. An exception is the possible dynamic instability of the M-80 in the subsonic region. It is not known whether this occurs for the other projectiles since they were not launched subsonically.

Weak dynamic instability in the subsonic region would not present a serious handicap to the flight characteristics of the M-80, or to the other projectiles. By the time subsonic velocities are reached, the projectile has already traveled about 800 meters and will have very nearly zero yaw. Consequently, considerable time (therefore, distance) will be required before the yaw will have a chance to become large enough to have a degrading influence on the flight behavior.

Values of the gyroscopic stability factor, s, were obtained for each round and are plotted versus Mach number in Figure A-6. The high values at about M = 2.8 were obtained by using a rifle with a 1 in 10 inch twist. These values have been converted to those that could be expected from a rifle with a 1 turn in 12 inches by multiplying by the ratio of the twists squared.

21

Since the curves do not represent the in-flight stability history
of the rounds, an example of such a history for the M-80 is shown in
Figure A-7. The curve represents a round launched at 2850 ft per sec.
The initial stability factor is 2.25 at 70°F; s increases throughout
its entire flight, but undergoes a change in its growth as the round
passes through Mach 1 due to a sudden drop in the drag. The curve
shows that the gyroscopic stability will never be worse than it is
immediately after launch.

C. Magnus Moment Derivative

The Magnus moment derivative, $C_{M_{p\alpha}}$, is plotted versus Mach number
in Figure A-8. All types behave roughly in the same manner. The shortest
round (M-80) has almost no moment, while the M-59 and M-61 (which differ
from the M-80 by body length only) have about the same values; these
values are both larger than those of the M-80. The M-62 values are still
higher; this is probably due to the even longer body. The Magnus
moment for all four types goes negative at $M = 1.5$ or slightly less.

D. Normal Force Coefficient and Center of Pressure

The normal force coefficient, C_{N_α}, is plotted versus Mach number
in Figure A-9 and the center of pressure is given in Figures A-10 and
A-11. The curves are well defined. The difference in drag between the
M-59 and the M-61 is again in evidence in the difference in C_{N_α} and CP_N.
Also evident is the fact that the effect of the tracer burning on these
two terms is insignificant.

22

REFERENCES

1. Kenneth Cobb. "Gun Settings for Side Firing Aircraft - 7.62 Minigun," AMR 65-24, July 1965.

2. Walter F. Braun, "The Free Flight Aerodynamic Range," Ballistic Research Laboratories Report No. 1048, July 1958.

3. Elizabeth R. Dickinson, "Physical Measurements of Projectiles," Ballistic Research Laboratories Technical Note 874, February 1954.

4. Charles H. Murphy, "Free Flight Motion of Symmetric Missiles," Ballistic Research Laboratories Report No. 1216, July 1963.

APPENDIX

PLOTTED CURVES FOR EXPERIMENTAL DATA

M-59(BALL)

M-80(BALL)
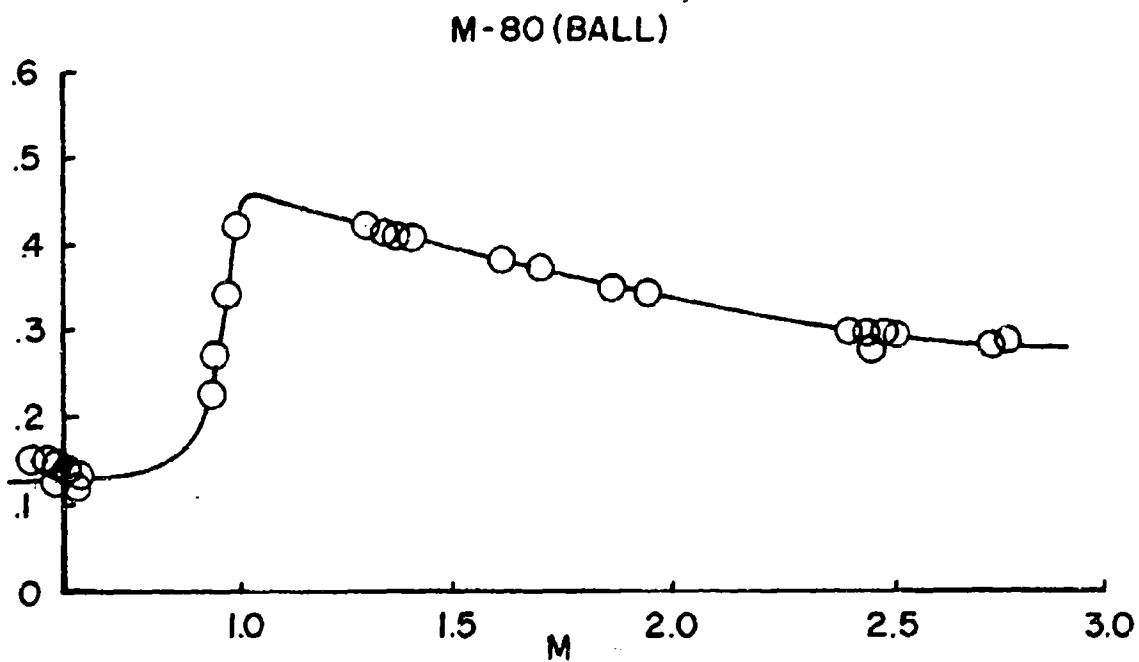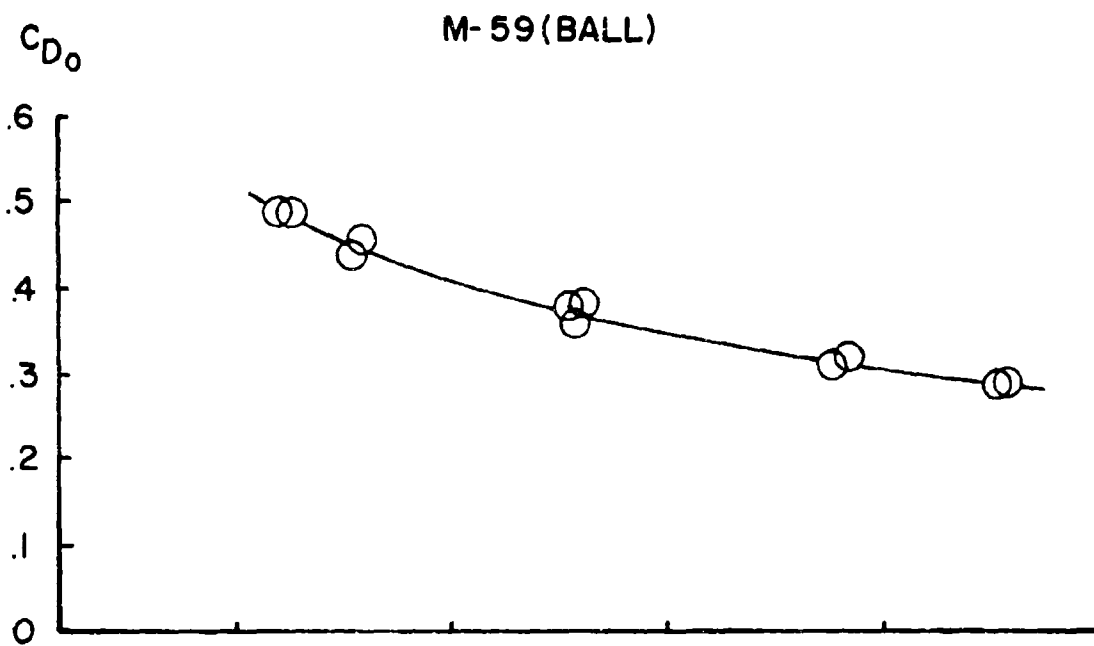
Figure A-1. Zero yaw drag coefficient vs mach number

27
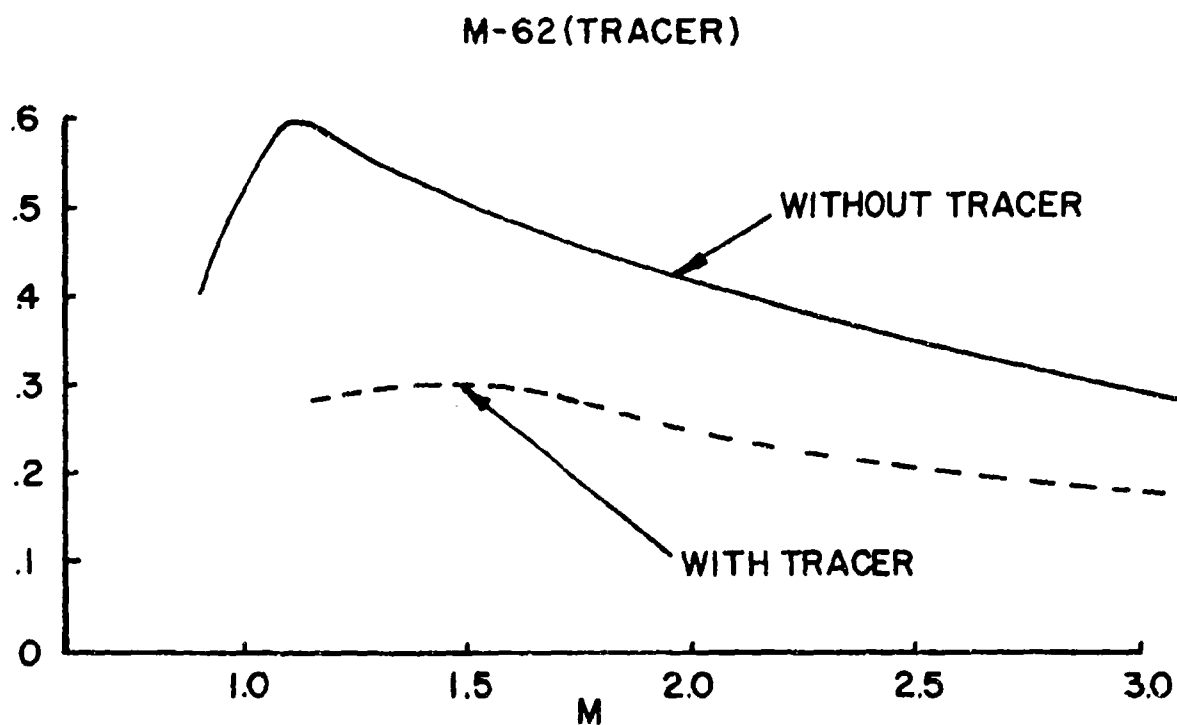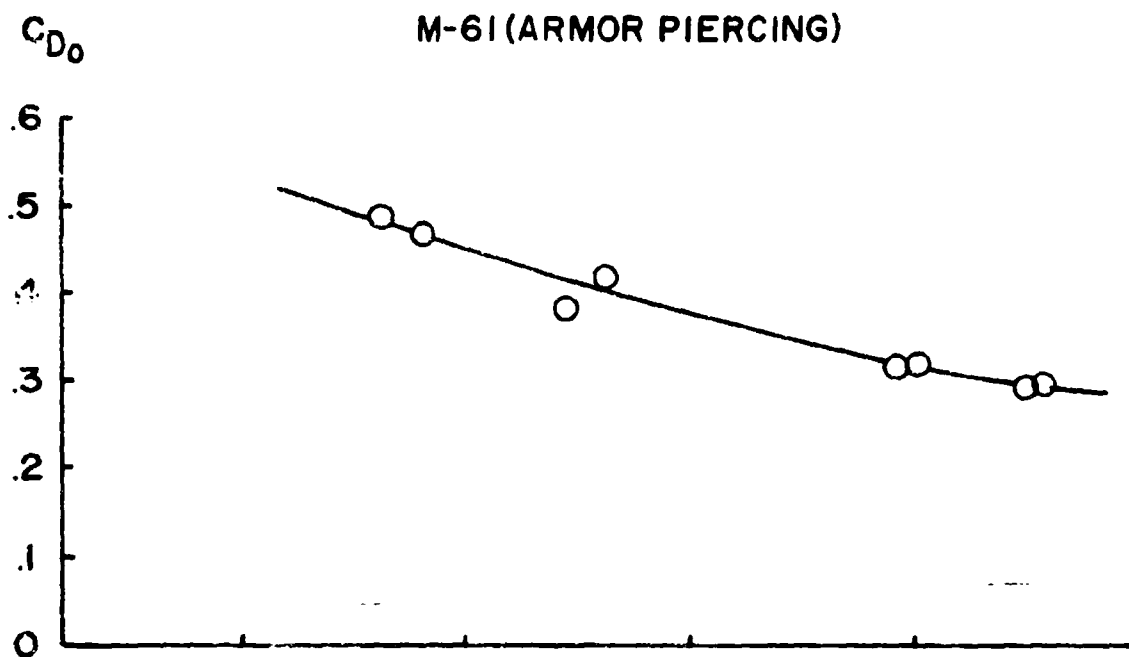
Figure A-2. Zero yaw drag coefficient vs mach number
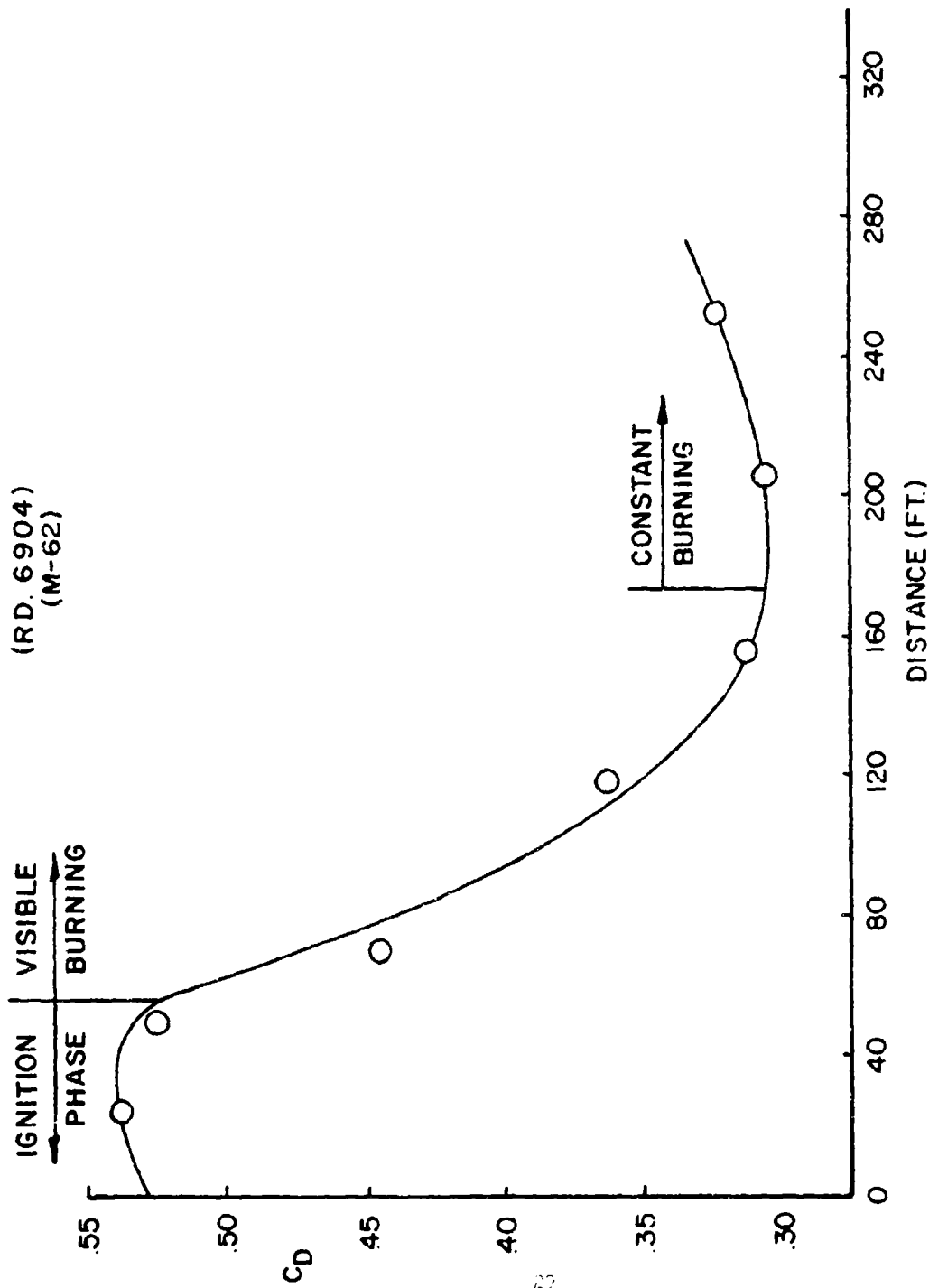
Figure A-3. Drag force coefficient vs distance
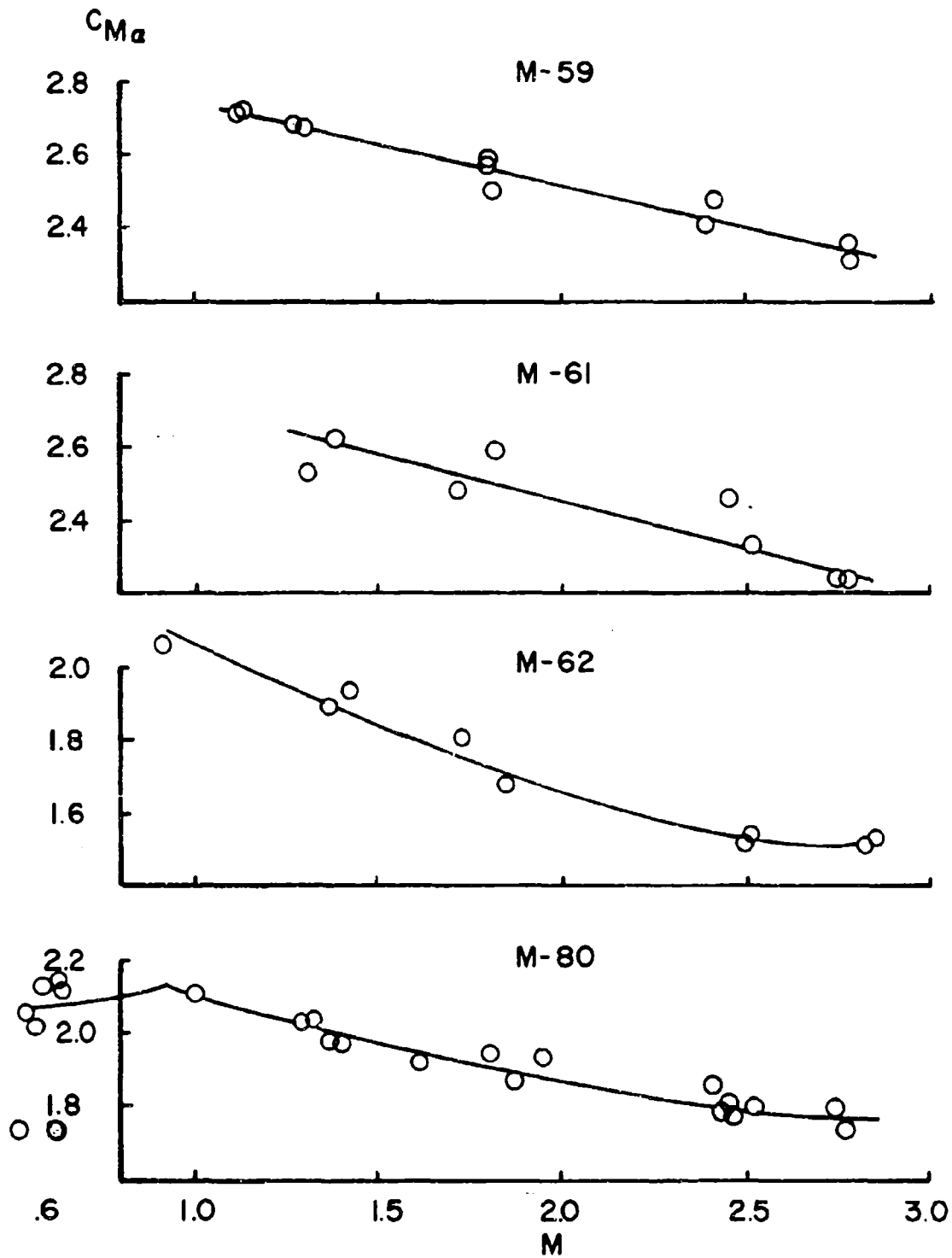
Figure A-4. Overturning moment derivative vs mach number
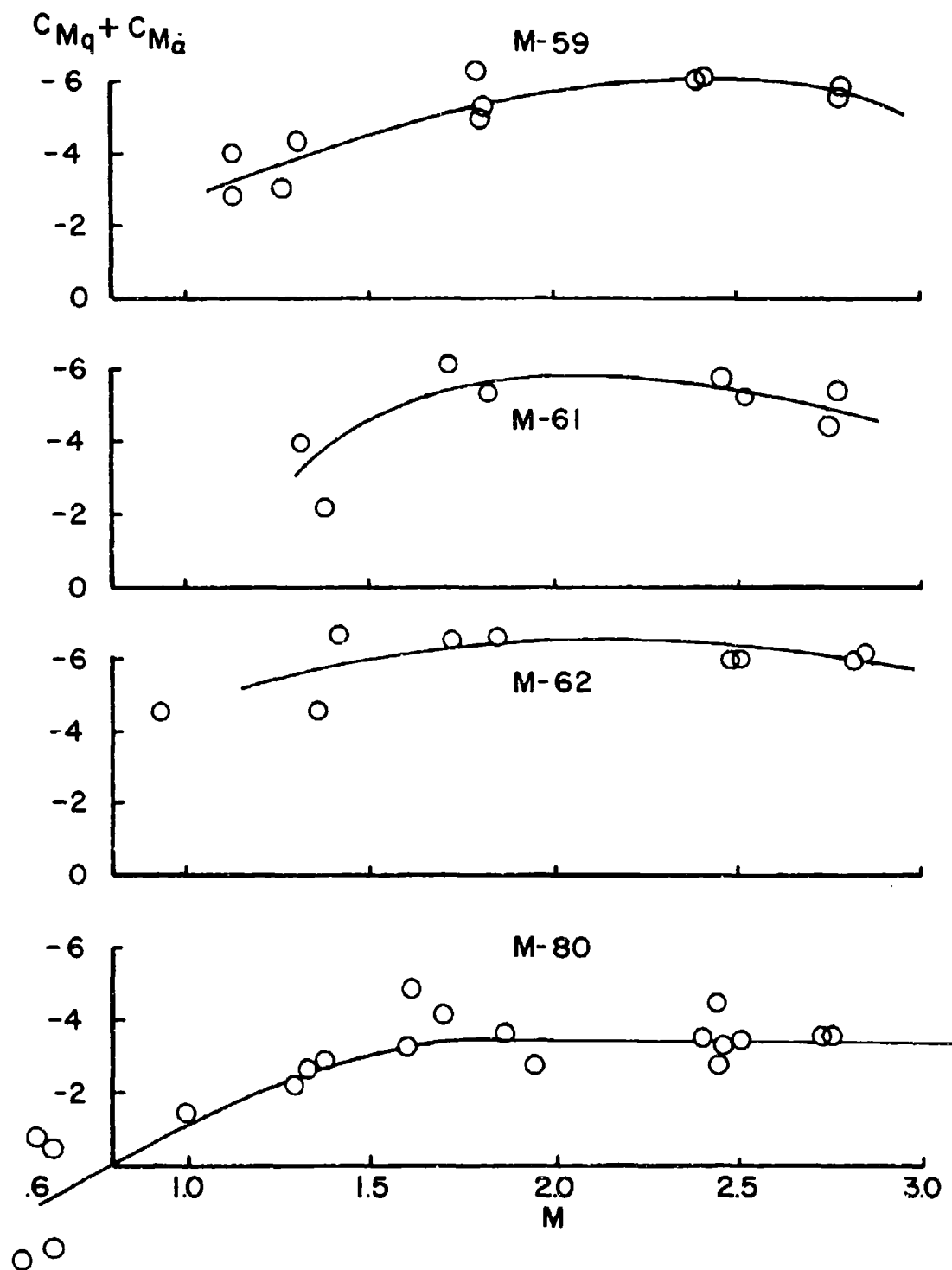
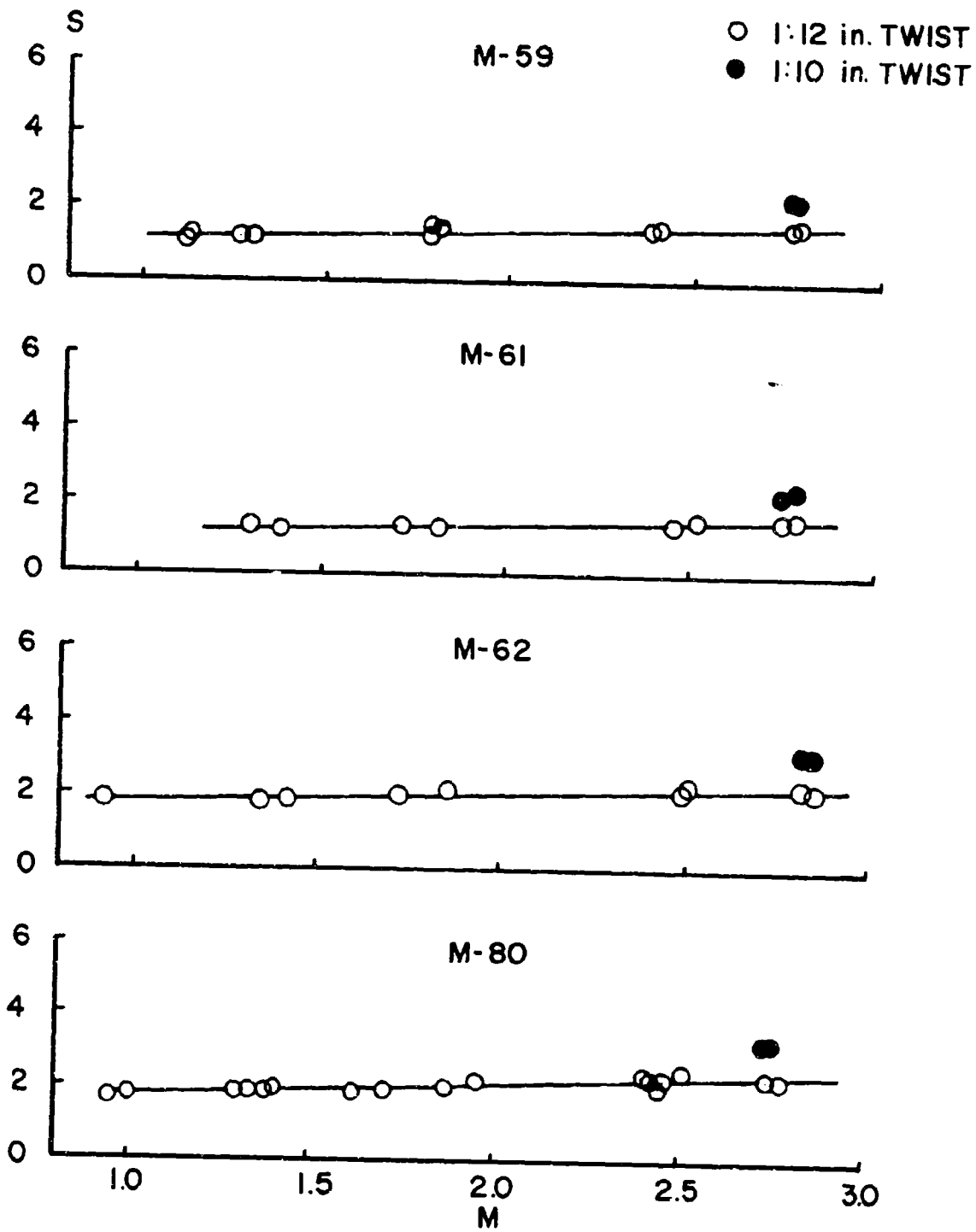Figure A-5. Damping moment derivatives vs mach number
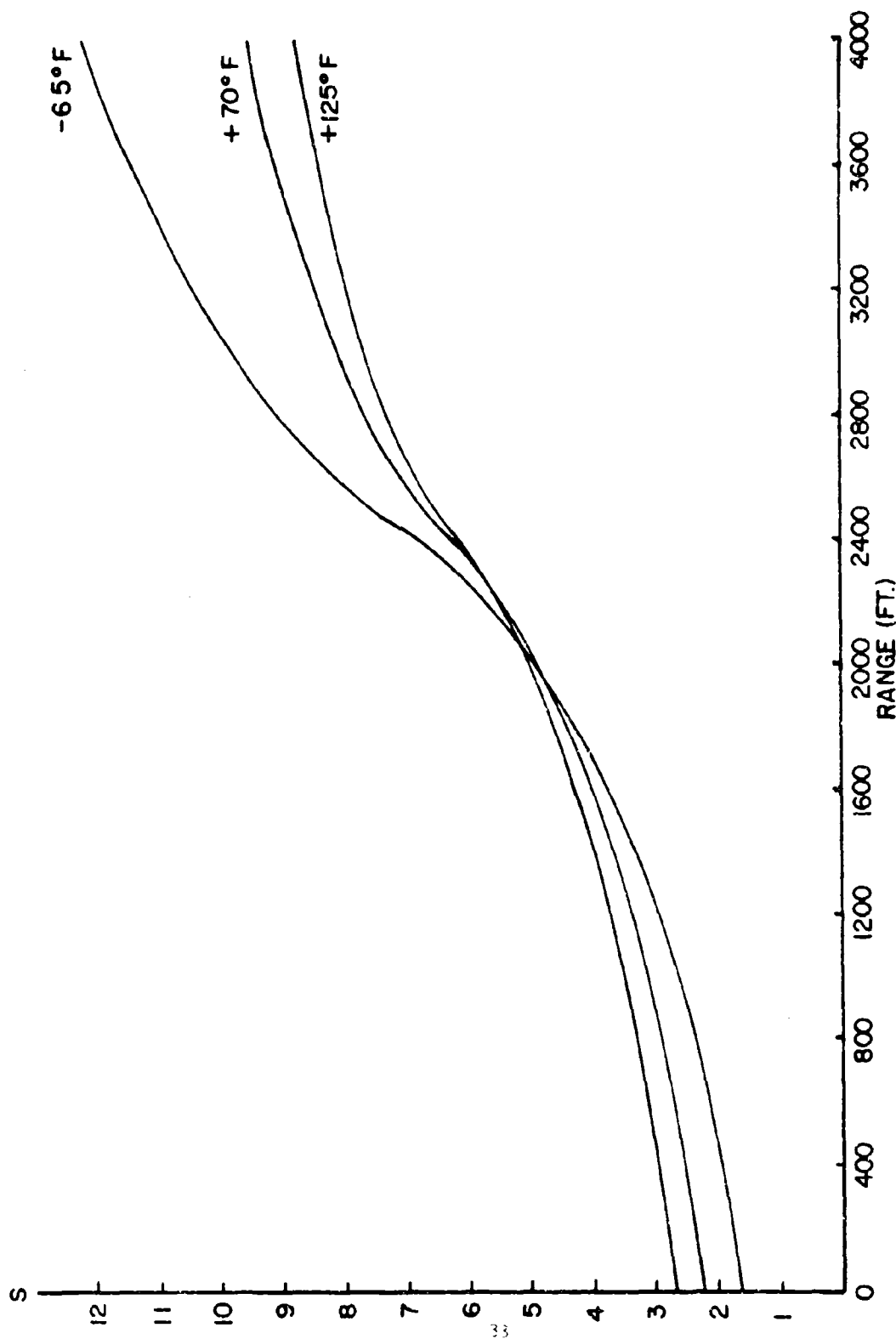
Figure A-6. Stability factor vs mach number

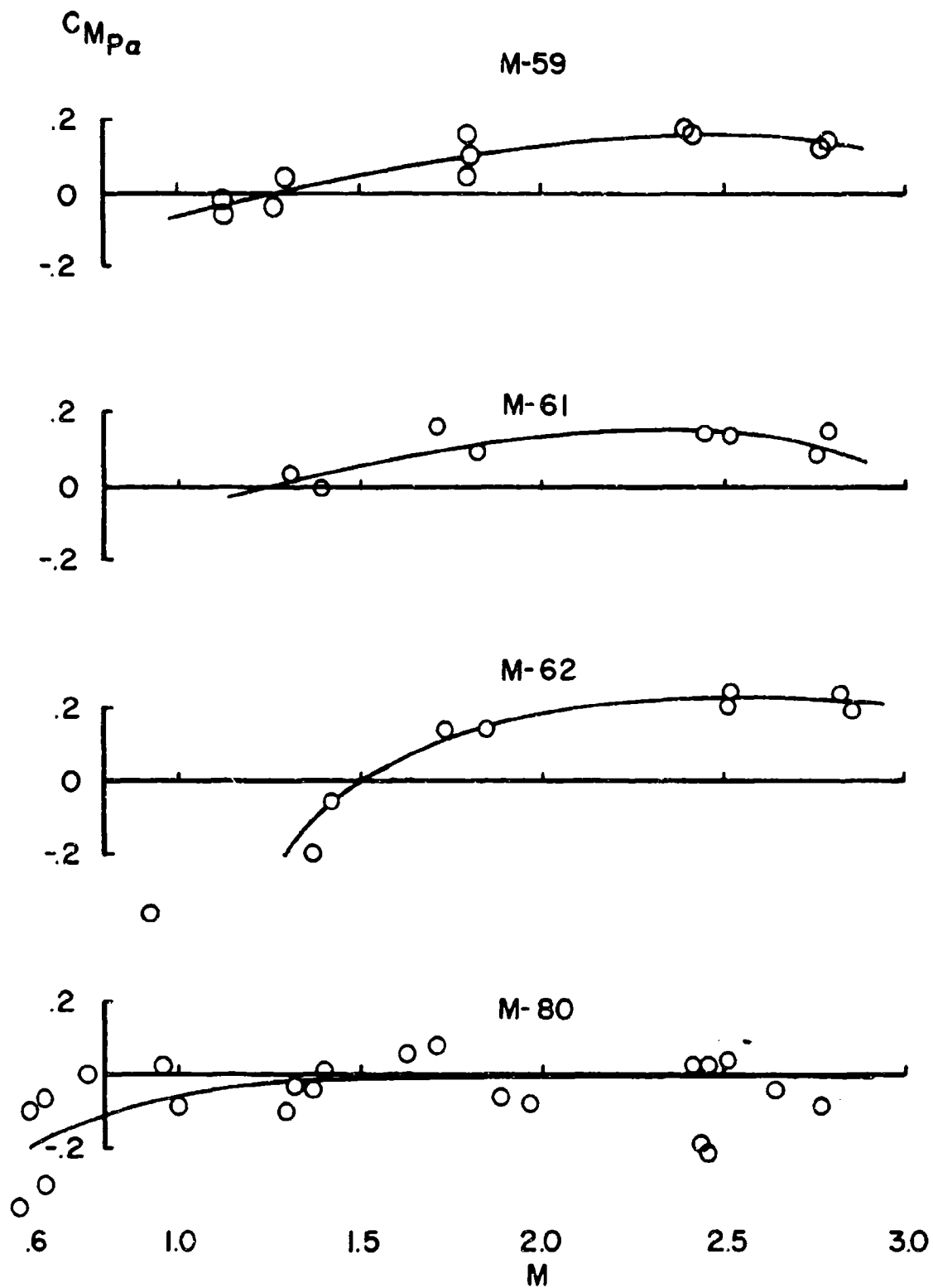Figure A-7. Stability factor vs range M-80 (1:12 in twist)

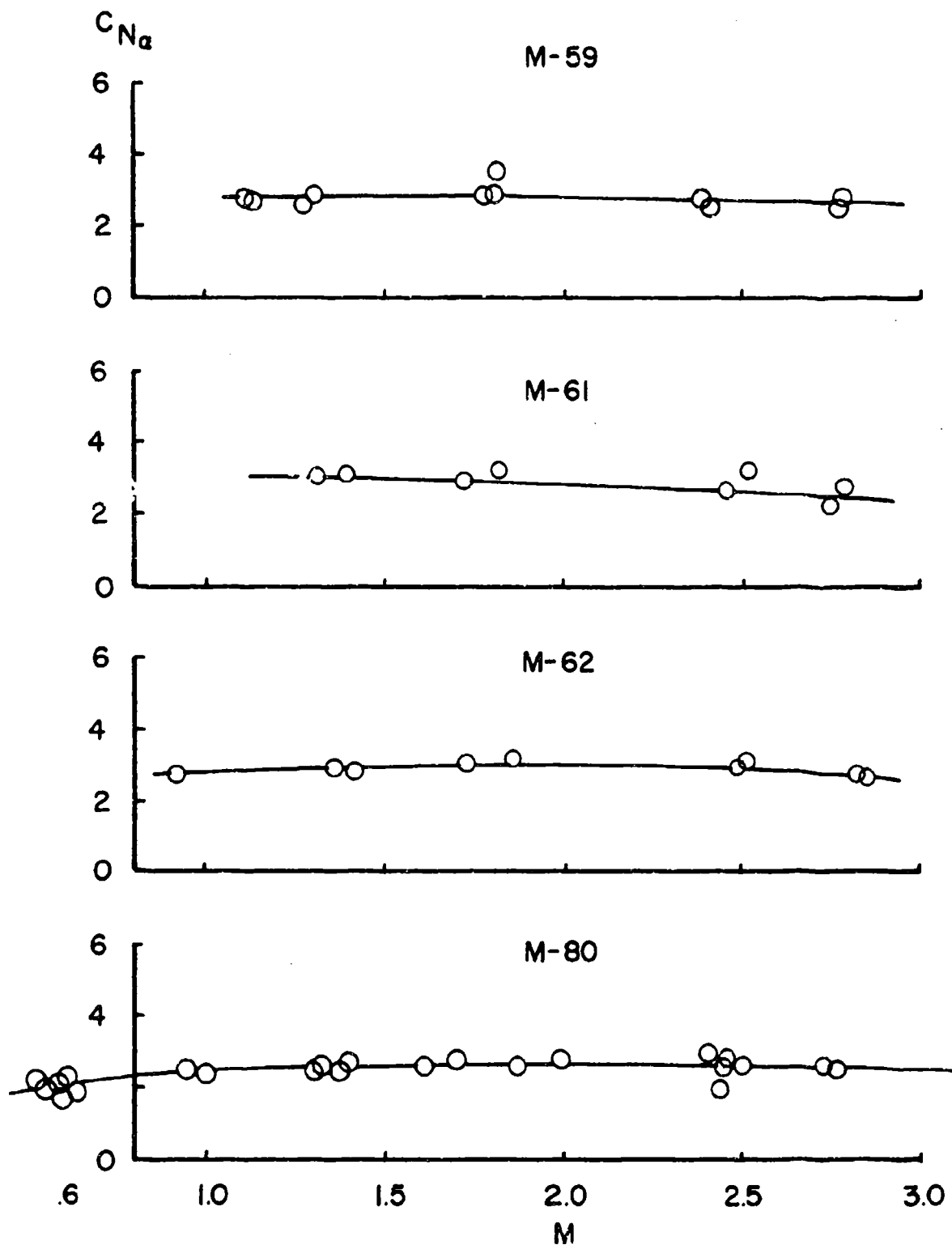Figure A-8. Magnus moment derivative vs mach number
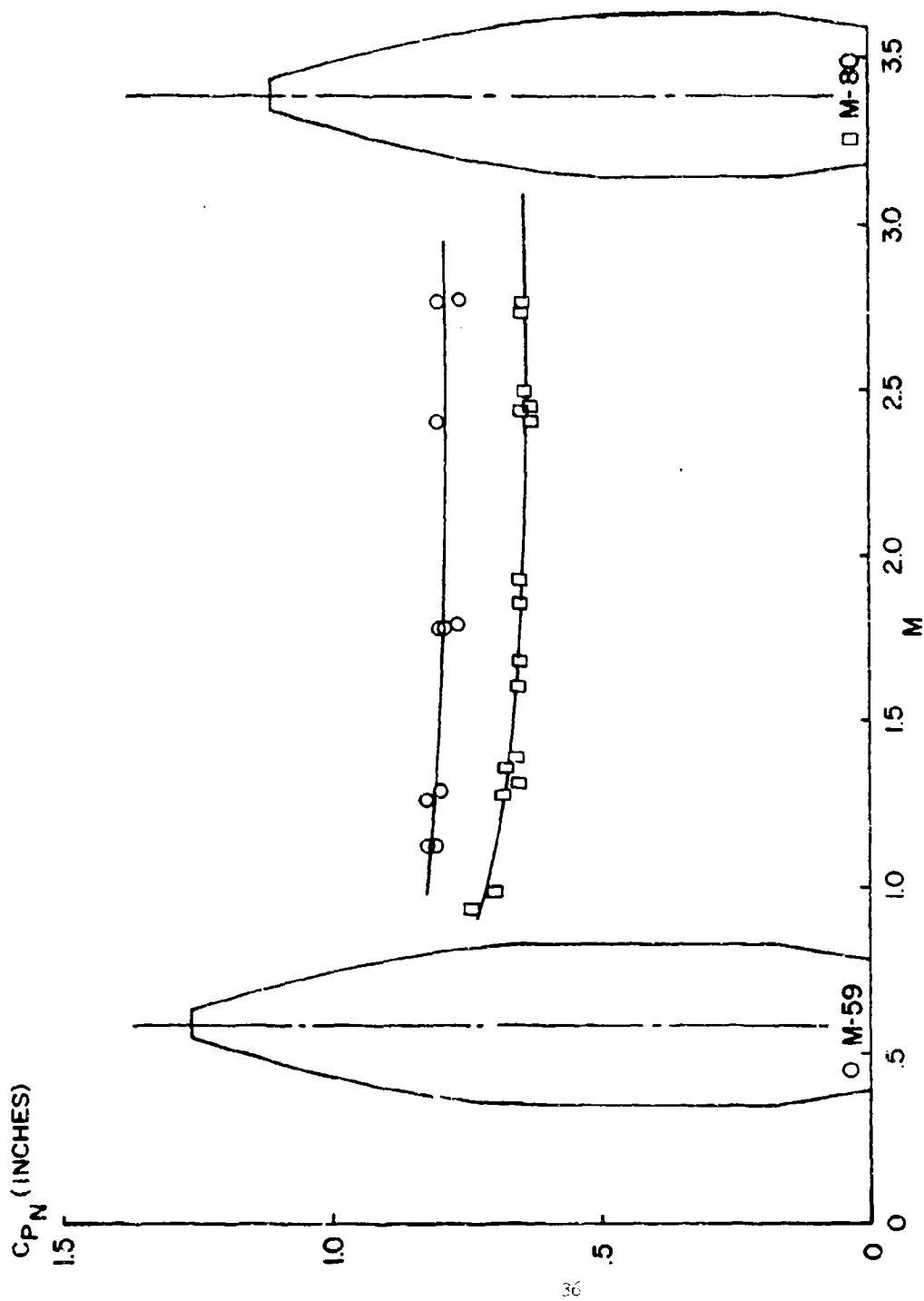
Figure A-9. Normal force coefficient vs mach number

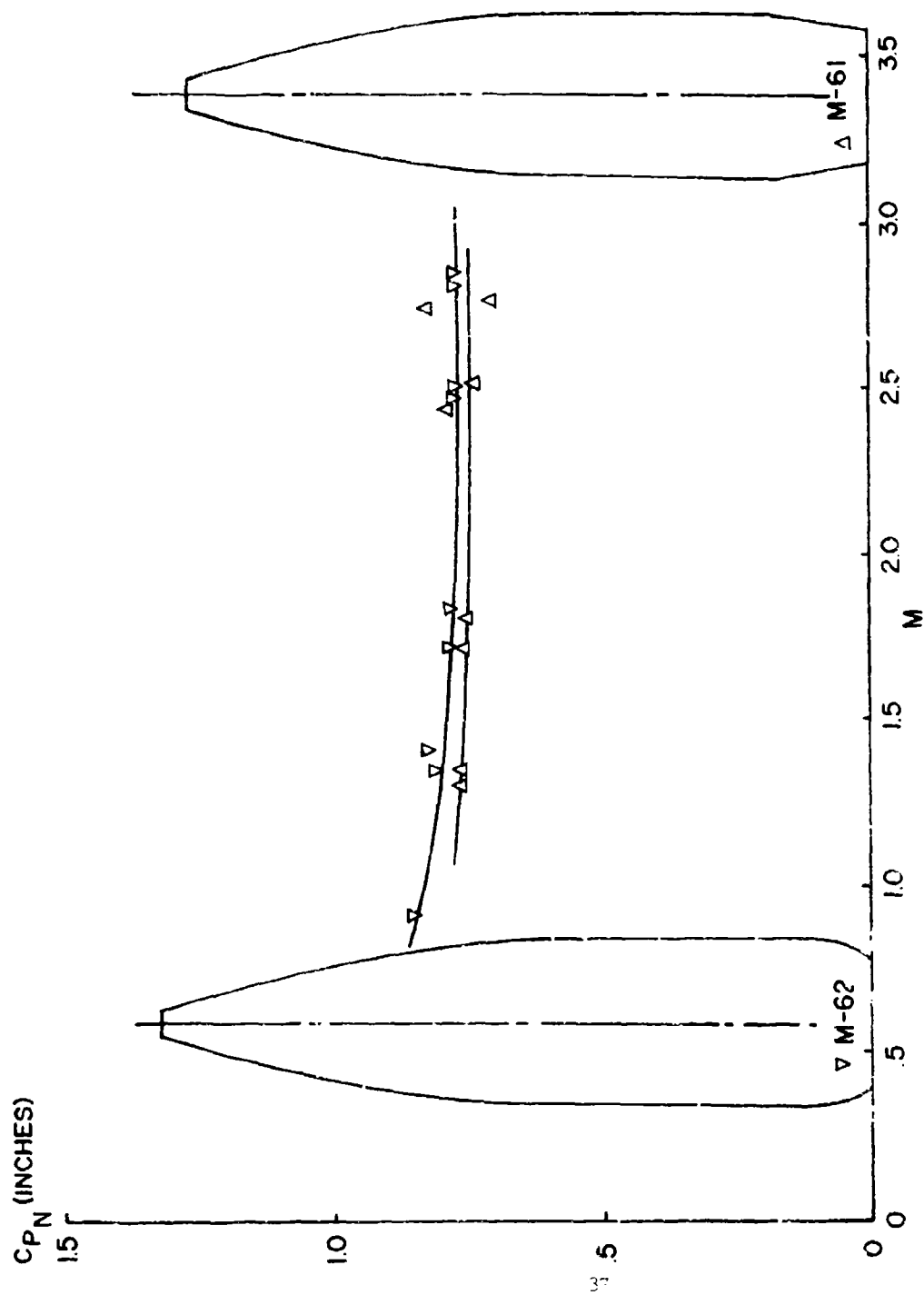Figure A-10. Center of pressure of the normal force vs mach number

Figure A-11. Center of pressure of the normal force vs mach number

DOCUMENT CONTROL DATA - R & D

(Security classification of title, body of abstract and indexing annotation must be entered when the overall report is classified)

1. ORIGINATING ACTIVITY (Corporate author)	2a. REPORT SECURITY CLASSIFICATION
U.S. Army Ballistic Research Laboratories Aberdeen Proving Ground, Maryland	Unclassified
	2b. GROUP

3. REPORT TITLE

AERODYNAMIC CHARACTERISTICS OF THE 7.62 MM NATO AMMUNITION M-59, M-80, M-61, M-62

4. DESCRIPTIVE NOTES (Type of report and inclusive dates)

5. AUTHOR(S) (First name, middle initial, last name)

Piddington, Maynard J.

6. REPORT DATE	7a. TOTAL NO. OF PAGES	7b. NO. OF REFS
March 1967	42	4
8a. CONTRACT OR GRANT NO.	9a. ORIGINATOR'S REPORT NUMBER(S)
b. PROJECT NO. RDT&E 1P014501A33D	Memorandum Report No. 1833
c.	9b. OTHER REPORT NO(S) (Any other numbers that may be assigned this report)
d.	

10. DISTRIBUTION STATEMENT

This document is subject to special export controls and each transmittal to foreign governments or foreign nationals may be made only with prior approval of Commanding Officer, U.S. Army Ballistic Research Laboratories, Aberdeen Proving Ground, Maryland.

11. SUPPLEMENTARY NOTES	12. SPONSORING MILITARY ACTIVITY
	U.S. Army Materiel Command Washington, D.C.

13. ABSTRACT

Tests have been conducted in the Free-Flight Aerodynamic Range on the NATO family of ammunition (M-80 ball, M-59 ball, M-62AP, and M-61 tracer). This report is the presentation and discussion of the data obtained in these tests. In general, the projectiles exhibited adequate gyroscopic and dynamic stability in the regions of probable use. The non-tracer members appear to have sufficiently similar drag properties to be adequate ballistic matches, while the tracer is not a match beyond about 600 meters.

14. KEY WORDS	LINK A		LINK B		LINK C	
	ROLE	WT	ROLE	WT	ROLE	WT
NATO Ammunition						
Exterior Ballistics						
Aerodynamic Characteristics						